Generation of infrared supercontinuum radiation: spatial mode dispersion and higher-order mode propagation in ZBLAN step-index fibers

Jacob Ramsay,[1] Sune Dupont,[2] Mikkel Johansen,[1] Lars Rishøj,[3] Karsten Rottwitt,[3] Peter Morten Moselund[4] and Søren Rud Keiding[1]*

[1]*Department of Chemistry, Aarhus University, DK-8000 Aarhus C, Denmark*
[2]*Department of Physics and Astronomy, Aarhus University, DK-8000 Aarhus C, Denmark*
[3]*DTU Fotonik, Department of Photonics Engineering, Tech. Uni. of Denmark, DK-2800 Kgs. Lyngby, Denmark*
[4]*NKT Photonics, Blokken 84, DK-3460 Birkerød, Denmark*
**keiding@chem.au.dk*

Abstract: Using femtosecond upconversion we investigate the time and wavelength structure of infrared supercontinuum generation. It is shown that radiation is scattered into higher order spatial modes (HOMs) when generating a supercontinuum using fibers that are not single-moded, such as a step-index ZBLAN fiber. As a consequence of intermodal scattering and the difference in group velocity for the modes, the supercontinuum splits up spatially and temporally. Experimental results indicate that a significant part of the radiation propagates in HOMs. Conventional simulations of supercontinuum generation do not include scattering into HOMs, and including this provides an extra degree of freedom for tailoring supercontinuum sources.

OCIS codes: (190.4370) Nonlinear Optics, fibers; (320.6629) Supercontinuum generation; (060.2270) Fiber characterization; (190.7220) Upconversion.

References and links

1. J. Dudley, G. Genty and S. Coen, "Supercontinuum generation in photonic crystal fiber," Rev. Mod. Phys. **78,** 1135 (2006).
2. R. R. Alfano and S. L. Shapiro, "Emission in the region 4000 to 7000 Å via four-photon coupling in glass," Phys. Rev. Lett., **24,** 584–587 (1970).
3. C. Kaminski, R. Watt, A. Elder, J. Frank, and J. Hult, "Supercontinuum radiation for applications in chemical sensing and microscopy," Appl. Phys. B: Lasers and Optics **92,** 367–378 (2008).
4. J. Mandon, E. Sorokin, I. T. Sorokina, G. Guelachvili and N. Picqué, "Supercontinua for high-resolution absorption multiplex infrared spectroscopy," Opt. Lett., **33**, 285–287 (2008).
5. S. A. Diddams, D. J. Jones, J. Ye, S. T. Cundiff, J. L. Hall, J. K. Ranka, R. S. Windeler, R. Holzwarth, T. Udem and T. W. Hänsch, "Direct link between microwave and optical frequencies with a 300 THz femtosecond laser comb," Phys. Rev. Lett., **84**, 5102–5105 (2000).
6. T. Udem, R. Holzwarth and T. W. Hansch, "Optical frequency metrology," Nature, **416**, 233–237 (2002).
7. S. Dupont, C. Petersen, J. Thøgersen, C. Agger, O. Bang and S. R. Keiding, "IR microscopy utilizing intense supercontinuum light source," Opt. Express, **20**, 4887–4892 (2012).
8. O. P. Kulkarni, V. V. Alexander, M. Kumar, M. J. Freeman, M. N. Islam, J. Fred, L. Terry, M. Neelakandan and A. Chan, "Supercontinuum generation from ∼1.9 to 4.5 μm in ZBLAN fiber with high average power generation beyond 3.8 μm using a thulium-doped fiber amplifier," J. Opt. Soc. Am. B **28**, 2486–2498 (2011).

#184533 - $15.00 USD Received 30 Jan 2013; revised 5 Apr 2013; accepted 9 Apr 2013; published 25 Apr 2013

9. C. Xia, M. Kumar, O. P. Kulkarni, M. N. Islam, J. Fred L. Terry, M. J. Freeman, M. Poulain and G. Mazé, "Mid-infrared supercontinuum generation to 4.5 μm in ZBLAN fluoride fibers by nanosecond diode pumping," Opt. Lett., **31**, 2553–2555 (2006).
10. C. Agger, C. Petersen, S. Dupont, H. Steffensen, J. K. Lyngsø, C. L. Thomsen, J. Thøgersen, S. R. Keiding and O. Bang, "Supercontinuum generation in ZBLAN fibers–detailed comparison between measurement and simulation," J. Opt. Soc. Am. B, **29**, 635–645 (2012).
11. G. P. Agrawal, *Nonlinear Fiber Optics*, 3rd ed.(Academic Press, 2001).
12. J. Dudley, X. Gu, L. Xu, M. Kimmel, E. Zeek, P. O'Shea, R. Trebino, S. Coen and R. Windeler, "Cross-correlation frequency resolved optical gating analysis of broadband continuum generation in photonic crystal fiber: simulations and experiments," Opt. Express, **10**, 1215–1221 (2002).
13. N. Akhmediev and M. Karlsson, "Cherenkov radiation emitted by solitons in optical fibers," Phys. Rev. A, **51**, 2602–2607 (1995).
14. F. Gan, "Optical properties of fluoride glasses - a review," J. of Non-Cryst. Solids, **184**, 9–20 (1995).
15. P. Hamm, "Coherent effects in femtosecond infrared spectroscopy," Chem. Phys., **200**, 415–429 (1995).
16. H. Harde, S. Keiding and D. Grischkowsky, "THz commensurate echoes: Periodic rephasing of molecular transitions in free-induction decay," Phys. Rev. Lett. **66**, 1834–1837 (1991).
17. F. Poletti and P. Horak, "Description of ultrashort pulse propagation in multimode optical fibers," J. Opt. Soc. Am. B, **25**, 1645–1654 (2008).
18. F. Poletti and P. Horak, "Dynamics of femtosecond supercontinuum generation in multimode fibers," Opt. Express **17** 6134–6147 (2009).
19. Y. Vidne and M. Rosenbluh, "Spatial modes in a PCF fiber generated continuum," Opt. Express, **13**, 9721–9728 (2005).
20. J. Cheng, M. E. V. Pedersen, K. Charan, K. Wang, C. Xu, L. Grüner-Nielsen and D. Jakobsen, "Intermodal Čerenkov radiation in a higher-order-mode fiber," Opt. Lett., **37**, 4410–4412 (2012).
21. M. Ziemienczuk, A. M. Walser, A. Abdolvand and P. S. J. Russell, "Intermodal stimulated Raman scattering in hydrogen-filled hollow-core photonic crystal fiber," J. Opt. Soc. Am. B, **29**, 1563–1568 (2012).

1. Introduction

In recent years, supercontinuum generation has been a field of great interest, and the physical processes involved in the generation have been studied vigorously (for a review, see [1]). Numerous applications have emerged since the first supercontinuum in bulk glass was reported by Alfano et al. [2], in such diverse fields as spectroscopy [3, 4] and optical metrology [5, 6]. Recently, supercontinua have been pushed into the mid-infrared, making room for new applications in spectroscopy and microspectroscopy [7–10], as the molecular fingerprint region can be reached. Novel soft glass fibers such as ZBLAN or chalcogenide are often used to be able to reach into the mid-infrared. Often microstructured fibers are used to tailor the dispersion profile to a specific pump wavelength and supercontinuum profile. However, ZBLAN fibers are not easily microstructured and to develop new fibers optimized for supercontinua generation, it is important to consider the generation process correctly. It is often assumed that the radiation is only propagating single-moded, and simulations are therefore carried out within this premise, i.e. the excitation of higher order spatial modes is not considered. The normalized frequency parameter V determines the number of modes that can propagate through the fiber at a given wavelength, and for step-index fibers, V is defined as [11]

$$V = \frac{2\pi a}{\lambda}\mathrm{NA} \tag{1}$$

where a is the fiber core radius, and NA is the numerical aperture. When $V < 2.405$, only the fundamental mode is supported by the fiber, and in this case of a 10 μm step-index fiber with $\mathrm{NA} = 0.2$, the cut-off wavelength is 2.6 μm. However, since the generation of infrared wavelengths depends on nonlinear mixing processes across the bandwidth of the supercontinuum, the influence of HOMs on the generation process must be considered.

Here, experiments are carried out to get a closer look at the temporal and spectral distribution of a supercontinuum generated in a step-index ZBLAN fiber. It is shown that even though the fiber is pumped above the cut-off wavelength of specific higher order spatial modes, these

#184533 - $15.00 USD Received 30 Jan 2013; revised 5 Apr 2013; accepted 9 Apr 2013; published 25 Apr 2013

modes are still excited as the supercontinuum is generated. This leads to significant delays between the radiation propagating in different modes, as a consequence of their different group velocities. This must therefore be considered, when modelling supercontinuum generation in multimoded fibers, or in pulse compression applications. The multimode propagation is also important if diffraction-limited focussing is desired.

The approach for investigating the temporal and spectral distribution of the supercontinuum is based on a crosscorrelation using sum frequency generation (SFG) in a nonlinear crystal [12]. By upconverting the entire supercontinuum with a femtosecond pulse, spectrograms are recorded that can reveal the propagation in higher-order modes.

2. Experimental setup

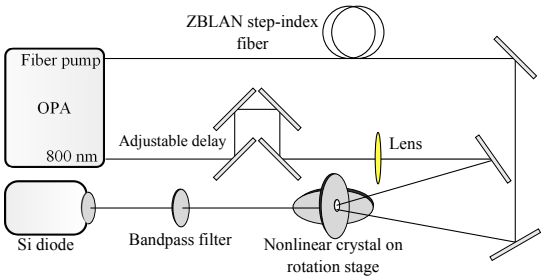

Fig. 1. Experimental setup.

A schematic overview of the setup is shown in Fig. 1. A 1 kHz Ti:sapphire system emitting 100 fs pulses with a pulse energy of 0.5 mJ is used to pump an OPA. The idler from the OPA is used to pump a 28 cm Fiberlabs ZBLAN fiber with a core diameter of 10.0 μm, and a numerical aperture of NA = 0.2. The fundamental mode has a zero dispersion wavelength close to 1.65 μm. In this setup, the fiber pumping power is adjusted using neutral density filters, to achieve typical pulse-energies of 100 nJ before coupling into the fiber. The autocorrelation of the idler from the OPA shows a temporal width of 75 fs. The resulting supercontinuum is passed through a 1 mm $LiIO_3$ crystal. The crystal is mounted on a rotation stage to be able to control the phase matching condition for sum frequency generation. Another arm with 800 nm fs pulses from the Ti:sapphire source is sent through a linear delay stage, and then passed through the $LiIO_3$ crystal as well. The signal is measured by a Si-diode. Since each wavelength of the supercontinuum is phase matched at a particular crystal angle, this angle can be used to measure the wavelength uniquely, thus no monochromator is needed. This measure of wavelength is calibrated by using a spectrometer to make sure the crystal angles correspond to the correct supercontinuum wavelengths. The spectral resolution is given by the phase matching bandwidth of the crystal, and differs over the spectral range covered by the supercontinuum. At 4 μm the phasematching bandwidth is approximately 0.3 μm, whereas it is only approximately 0.03 μm at 2 μm. The resolution on the time axis of the spectrograms is limited by the temporal width of the 800 nm upconversion pulse.

3. Results

Supercontinua are commonly described using the generalized nonlinear Schrödinger equation (GNLSE), accounting for the important processes that act together to constitute the generation process [1, 11]. The dispersion profile of the fiber is of major importance, and pumping at wavelengths in the anomalous dispersion regime will allow soliton dynamics to be a governing

#184533 - $15.00 USD Received 30 Jan 2013; revised 5 Apr 2013; accepted 9 Apr 2013; published 25 Apr 2013

phenomenon in the generation process. The soliton number N is given by

$$N^2 = \frac{\gamma P_0 T_0^2}{|\beta_2|}, \tag{2}$$

where γ is the nonlinear parameter, P_0 is the peak power, T_0 is the temporal width, and β_2 is the group velocity dispersion parameter. The soliton number becomes larger when pumping near the ZDW in the anomalous dispersion regime. A high soliton number and pumping near the ZDW facilitates radiation into the normal dispersion regime through emission of dispersive waves [11, 13]. The dispersive wave generation relies on a soliton fission causing emission of these waves, which extend into the region of normal dispersion. When pumping close to the ZDW the phase matched wavelengths will be spectrally closer to the soliton spectrum giving better overlap. In addition, solitons created through soliton fission close to the ZDW are temporally shorter and thus spectrally broader and with higher peak power, providing higher gain for the dispersive waves. Therefore, the supercontinuum is expected to be spectrally broad when the soliton number is high. In this case, the fiber is pumped by free space coupling with pulse energies of approximately 30 nJ (including coupling losses), centered at 1.8 μm. With a ZDW at 1.65 μm, the soliton number is calculated to be approximately 20. This is based on material dispersion parameters provided by [14], Gan *et. al*, and the waveguide dispersion was found using calculations from [10], Agger *et. al*. The spectrum of the generated supercontinuum is

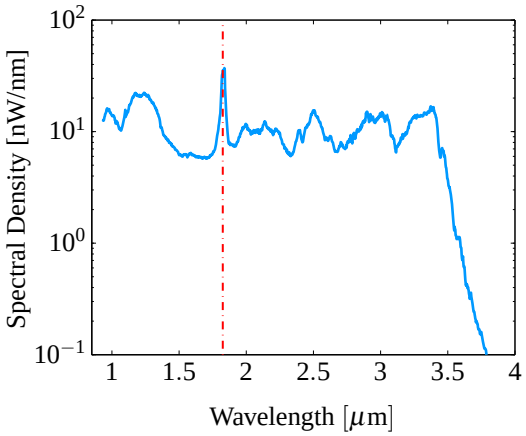

Fig. 2. Spectrum of the supercontinuum. The fiber is pumped with a central wavelength at 1.8 μm (red dashed line), with pulse energies of 30 nJ, including coupling losses.

measured using a monochromator, and is seen in Fig. 2. This spectrum is broad as expected, and correspond well to [10], Agger *et. al*.

The corresponding spectrogram from the crosscorrelation of this supercontinuum is seen in Fig. 3(a). It is seen that the spectral features in the spectrogram correspond qualitatively well to the measured spectrum, spanning from 0.8 μm to 3.5 μm. The leading edge of the pulse is seen at 0 ps. The supercontinuum is split up temporally, especially in the short wavelength region of the spectrum. This clearly indicates that HOMs have been excited, and since these modes have different group velocity dispersion, temporal splitting occurs. The impact of input polarization on the spectrograms has been investigated. No changes in the spectrogram were observed when turning the input end of the fiber without changing the polarization of the pump laser. A half-wave plate was furthermore introduced to the supercontinuum to turn the polarization. This did not change the spectrograms in any way, indicating that the supercontinuum is unpolarized, since the SFG crystal acts as a polarizer. In Fig. 3(b), another spectrogram is shown, pumping at

#184533 - $15.00 USD Received 30 Jan 2013; revised 5 Apr 2013; accepted 9 Apr 2013; published 25 Apr 2013

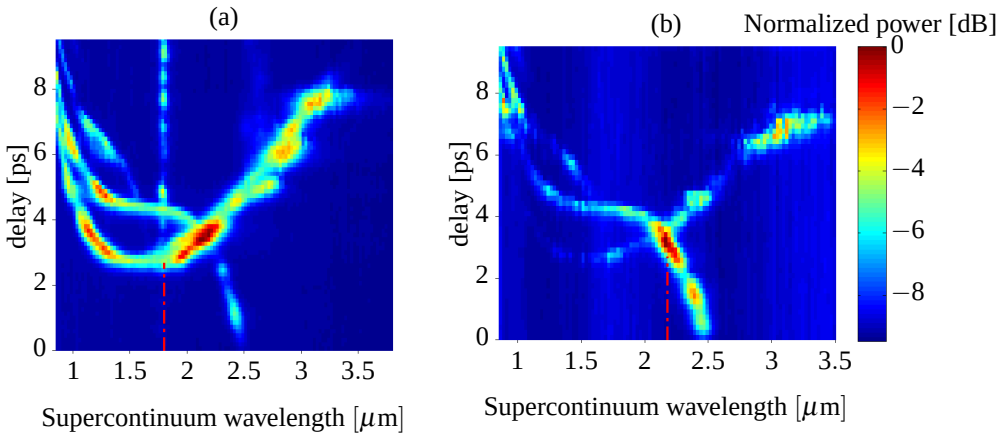

Fig. 3. Spectrograms resulting from the crosscorrelation are obtained by changing crystal phase matching angle. The fiber is pumped with a central wavelength of (a) 1.8 μm and (b) 2.2 μm, respectively (red dashed lines). The intensities are plotted on a dB scale. The pulse energy including coupling losses is in both cases approximately 30 nJ

2.2 μm. Here it is evident that the supercontinuum is not broadened as efficiently, as expected since the pump is further away from the ZDW, giving a lower soliton number of approximately 8. When pumping at 1.8 μm, a range of strong echoes trailing the main pulse are seen. When the pump wavelength is moved to 2.2 μm, these echoes are absent. When pumping at 2.6 μm (not shown) the echoes appear again. This is identified as free induction decay in the atmosphere [15, 16], as water has a strong absorption line at around 1.8 μm, and the pump propagates approximately 3 m in free space. This effect is absent at 2.2 μm, as the absorption in the atmosphere is low at this wavelength, and is seen again (not shown) when pumping at 2.6 μm, due to a combination of H_2O and CO_2 absorption lines.

4. Discussion

A discussion of the temporal and spectral distribution of the supercontinuum is provided in this section. It is important to consider how the radiation is scattered into the higher-order modes to understand the resulting spectrograms. The propagation of a supercontinuum in higher-order modes has earlier been discussed in detail in the context of simulations [17, 18]. Simulations are carried out using the multi-mode variant of the GNLSE (MM-GNLSE) in [18]. This approach requires complex computer simulations, and restrictions due to computation time apply, hence numerical approximations are necessary. Here, in order to get further insight into the mode scattering process, the expected arrival time for each wavelength component of the supercontinuum is calculated using the group velocity of the particular mode that the radiation propagates within. The arrival times are expected to follow this group delay, reported earlier for propagation in the fundamental mode in [12]. Therefore, this qualitative and simple analysis for identification of the excited modes is useful, based on a model, where the pulse is fully broadened into its spectral components instantaneously at the input end of the fiber, and then propagates in the first 6 modes with their group velocity along the entire fiber length. This is a good assumption, as the soliton fission distance L_{fiss} [1] is only 3-4 cm, and the change in the dispersion of the arrival times is comparable to the resolution of the experiment. The resulting calculations are shown along with the experimental data in Fig. 4(a). The ZBLAN index profile is calculated on the basis of the Sellmeier equations provided by Gan et. al. [14] combined with the waveguide dispersion.

#184533 - $15.00 USD Received 30 Jan 2013; revised 5 Apr 2013; accepted 9 Apr 2013; published 25 Apr 2013

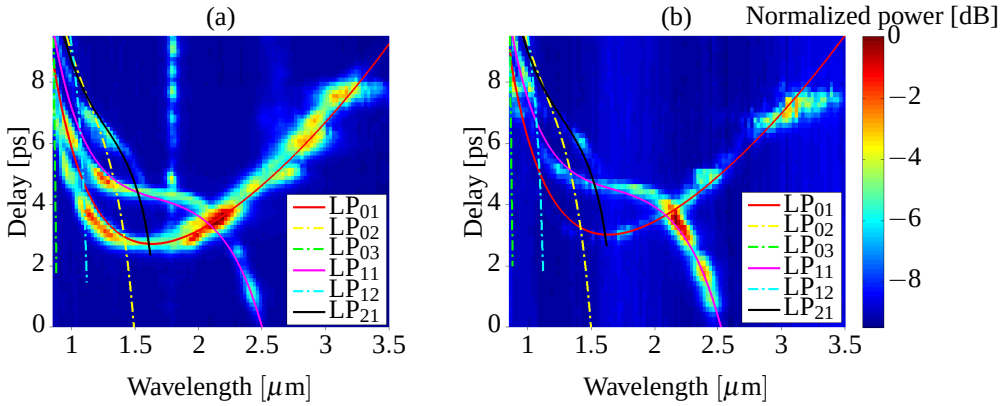

Fig. 4. The spectrograms from Fig. 3 plotted with arrival time calculations for the LP_{01}, LP_{11} and LP_{21} modes. The spectrograms are in good agreement with the calculated arrival times. (a) Pump at 1.8 μm (b) Pump at 2.2 μm. The intensities are plotted on a dB scale.

From Eq. (1), the fiber is single-moded for wavelengths longer than 2.6 μm. It is clearly seen that above this wavelength, the supercontinuum is only propagating in the fundamental mode. Therefore this mode is identified as the LP_{01} mode, and the zero dispersion wavelength for the fundamental mode is found to be around 1.65 μm as expected. Furthermore, integration across the spectrogram shows that approximately 40 % of the energy is propagating in other modes than the fundamental mode. It is evident from Fig. 4 that the excited modes are LP_{01}, LP_{11} and LP_{21}. These modes are excited exclusively, and excitation of the LP_{02} and LP_{03} modes was not observed. In order to exclude propagation in HOMs due to excitation caused by direct coupling of pump radiation into these modes, the fiber is pumped at 2.2 μm. The LP_{21} mode is excited even when pumping above the cut-off wavelength of this mode, as seen in Fig. 4(b). Therefore, the excitation of the LP_{21} mode is due to an intermodal scattering process in the fiber, as it is not possible to couple into this mode at 2.2 μm. As also observed in [18, 19], the excitation of HOMs is inevitable when dealing with high-power supercontinuum generation in fibers where HOMs are supported.

Several situations are considered in [18], pumping in various modes and allowing different mode coupling mechanisms to be present. When pumping in the fundamental mode of the fiber, four-wave mixing (FWM) into modes of the same symmetry class is found to be dominant. In particular, when pumping in the anomalous dispersion regime, radiation on the short-wavelength side of the ZDW is emitted by the solitons created from the soliton fission process. This phenomenon is known as emission of dispersive waves. Emission of intermodal dispersive waves has previously been reported experimentally [20]. The transfer of radiation into higher-order modes happens along the fiber, and is governed by a group velocity matching condition (or soliton trapping, [11]) for this process. This makes the dispersive wave from a given soliton travel at the same speed as the soliton. In this way, the time structure is well-defined to each mode and follows the group velocity, even though the intermodal scattering happens along the fiber, as the supercontinuum is broadening spectrally. The probability of the intermodal scattering process by emission of dispersive waves is dependent on the electric field overlap integral, and certain combinations of intermodal scattering are not allowed, depending on the angular symmetry of the modes. To scatter into the LP_{11} mode from the LP_{01} mode, the overlap integral $f_{01,01,01,11}$ (for four-wave mixing between 3 LP_{01} and one LP_{11} photon) can be

#184533 - $15.00 USD Received 30 Jan 2013; revised 5 Apr 2013; accepted 9 Apr 2013; published 25 Apr 2013

written as [11, 17, 20]

$$f_{01,01,01,11} = \frac{\langle F_{01}^* F_{01}^* F_{01} F_{11} \rangle}{[\langle |F_{01}|^2 \rangle \langle |F_{01}|^2 \rangle \langle |F_{01}|^2 \rangle \langle |F_{11}|^2 \rangle]^{1/2}} \tag{3}$$

where F_{kl} is the spatial distribution of fiber mode LP_{kl}, and the angle brackets denote integration over the transverse coordinates. As LP_{01} and the LP_{11} modes belong to different symmetry classes, the spatial overlap integral $f_{01,01,01,11}$ is zero for a perfect cylindrical fiber symmetry. This strict selection rule for intermodal scattering by dispersive waves could be relaxed by imperfections in the fiber. However, in the fiber used in our experiments, an argument against this process is made, as experiments with fiber bending did not change the spectrogram in any way, even though this changes the overlap integral [20].

A situation where the two modes LP_{01} and LP_{11} are both excited when coupling into the fiber is now considered. In relation to the simulations in [18], pumping different symmetry classes adds complexity to the system, allowing FWM and cross-phase modulation (XPM) to transfer energy between all existing modes, regardless of the previously mentioned symmetry considerations. XPM was also shown in [18] to be important in the broadening of the spectrum in the HOMs, when radiation is present in more than one mode. This situation cannot be ruled out completely, though thorough experimental efforts to couple into the fundamental mode only have been made.

Considering a final mechanism, Raman scattering could potentially scatter into higher order modes, as previously reported in [21] for a hydrogen-filled hollow-core photonic crystal fiber. This requires spatial intensity overlap. The overlap integral $f_{01,11}$ for Raman scattering from LP_{01} into LP_{11} can be written as [11]

$$f_{01,11} = \frac{\langle |F_{01}|^2 |F_{11}|^2 \rangle}{\langle |F_{01}|^2 \rangle \langle |F_{11}|^2 \rangle}, \tag{4}$$

where F_{kl} is the transverse distribution of fiber mode LP_{kl}. The angle brackets denote integration over the transverse coordinates. Calculations of the effective area (which is the inverse overlap integral for Raman scattering [11]) between the fundamental and the HOMs considered in this paper are shown in Fig. 5.

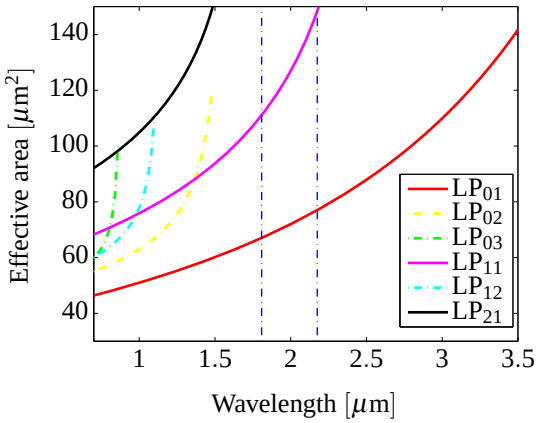

Fig. 5. Effective areas (inverse overlap integrals $1/f_{01,xy}$, where LP_{xy} is given by legend) for Raman scattering into 6 modes from the LP_{01} mode. The blue dashed lines are the pump wavelengths used for the upconversion experiments.

#184533 - $15.00 USD Received 30 Jan 2013; revised 5 Apr 2013; accepted 9 Apr 2013; published 25 Apr 2013

It is seen that intramode scattering has the best overlap (Raman scattering from the fundamental mode into itself), but intermodal scattering is indeed possible. The overlap integral between the LP_{01} and the two modes that are actually excited (LP_{11} and LP_{21}) is slightly smaller than that of the LP_{02}, LP_{03} and LP_{12} modes, though it is noted that since the excited modes have the highest cut-off wavelengths of the HOMs, they are the first modes available for scattering into as the pump spectrum broadens early in the fiber. The effective areas of the HOMs are comparable to that of the fundamental mode and one must also consider nonlinear broadening effects in the HOMs themselves. However, as evident from Fig. 4, the slope of the calculated group delays in the HOMs are all negative, corresponding to normal dispersion in the HOMs. This will restrict the non-linear broadening mechanisms to Raman scattering and self-phase modulation.

It is clear that multi-mode supercontinuum generation is very complex. When looking at the intensities in the spectrogram, it can be argued that maximum intensities correspond to solitons in the anomalous dispersion regime of the fundamental mode, which are in turn matched in group velocity with maximum intensities in the normal dispersion regime, corresponding to a soliton-trapped dispersive wave at delays of around 3 ps. The wavelengths of the dispersive wave can be calculated [11], and when pumping at 1.8 μm and 2.2 μm, the corresponding dispersive waves are generated at 1.24 μm and 0.98 μm in the LP_{01} mode, respectively. This corresponds well to the observed maximum intensities in the fundamental mode, seen in the spectrograms in Fig. 3 for both pump wavelengths. The overlap integral for intermodal scattering from LP_{01} to LP_{11} is zero, and therefore initial Raman scattering into this mode is likely, transferring energy into both symmetry groups. This is followed by complex scattering mechanisms such as FWM and XPM between the excited modes, as the symmetry restrictions are removed.

To conclude, femtosecond upconversion of an infrared supercontinuum generated in a step-index ZBLAN fiber is used to obtain detailed spectrograms. The upconversion technique may be used for measuring the group velocity dispersion in soft-glass fibers. It has been shown that radiation can be scattered into higher order modes as the supercontinuum broadens, even when pumping above the cut-off wavelength of a given mode. The modes are identified by calculating arrival times at the fiber end according to the group velocity. These arrival times are in good agreement with the crosscorrelation measurements. A discussion of the possible intermodal scattering mechanisms reveals that supercontinuum scattering into HOMs is very complex, and a combination of effects including Raman scattering, FWM and XPM are likely to scatter into the HOMs. The LP_{11} and LP_{21} modes are excited exclusively, though other modes such as the LP_{02} and LP_{03} modes exist in the wavelength region of interest. The supercontinuum breaks up into multiple pulses, and a temporal separation occurs due to the significant difference in group velocity dispersion of the excited modes. For many applications, such as time resolved experiments, or for diffraction limited focussing, it is very important that these dynamics take place, and they must therefore be considered. Approximately 40 % of the supercontinuum radiation is propagating in HOMs. As fiber drawing and tailoring improves, this may be used as an extra degree of freedom for optimization of supercontinuum sources.

#184533 - $15.00 USD Received 30 Jan 2013; revised 5 Apr 2013; accepted 9 Apr 2013; published 25 Apr 2013